Chinese Chemical Letters 33 (2022) 1313–1316

Contents lists available at ScienceDirect

Chinese Chemical Letters

journal homepage: www.elsevier.com/locate/cclet

# Achieving simultaneous Cu particles anchoring in meso-porous $TiO_2$ nanofabrication for enhancing photo-catalytic $CO_2$ reduction through rapid charge separation

Jinyan Xiong[a], Mengmeng Zhang[b], Mengjie Lu[a], Kai Zhao[c], Chao Han[d], Gang Cheng[b], Zhipan Wen[b,*]

[a] College of Chemistry and Chemical Engineering, Hubei Key Laboratory of Biomass Fibers and Ecodyeing & Finishing, Wuhan Textile University, Wuhan 430200, China
[b] School of Chemistry and Environmental Engineering, Wuhan Institute of Technology, Wuhan 430205, China
[c] School of Materials Science and Energy Engineering, Foshan University, Foshan 528000, China
[d] Australia School of Civil and Environmental Engineering, Faculty of Engineering and Information Technology, University of Technology Sydney, Sydney, NSW 2007, Australia

ARTICLE INFO

*Article history:*
Received 26 May 2021
Revised 20 June 2021
Accepted 24 July 2021
Available online 30 July 2021

*Keywords:*
$TiO_2$
Copper
Photo-catalytic $CO_2$ reduction
Photo-catalysis
Charge separation
Schottky junction

ABSTRACT

A facile solvo-thermal approach was successfully employed to prepare titanium oxide ($TiO_2$) nano-aggregates with simultaneous copper particles anchoring. The as-synthesized composite could convert $CO_2$ into $CH_4$ and CO products under simulated solar irradiation. The impact of copper loading amounts on the photo-reduction capability was evaluated. It was found proper amount of Cu loading could enhance the activity of $CO_2$ photo-reduction. As a result, the optimal composite ($TiO_2$-Cu-5%) consisting of $TiO_2$ supported with 5% (mole ratio) Cu exhibits 2.2 times higher $CH_4$ yield and 3 times higher CO yield compared with pure $TiO_2$. Conduction band calculated from the band gap and valence X-ray photoelectron spectroscopy (XPS) indicated $TiO_2$ nano-aggregates have suitable band edge alignment with respect to the $CO_2/CH_4$ and $CO_2$/CO redox potential. Furthermore, with involving of Cu particles, an efficient separation of photo-generated charges was achieved on the basis of photocurrent response and photoluminescence spectra results, which contributed to the improved photo-catalytic performance. The present work suggested that the Cu-decorated $TiO_2$ could serve as an efficient photo-catalyst for solar-driven $CO_2$ photo-reduction.



Overcoming the current challenge of energy crisis and climate change resulting from excessive fossil fuels combustion along with $CO_2$ emissions has attracted great attention. Semiconductor photo-catalysis, especially solar-driven photo-catalytic $CO_2$ reduction, was regarded as one of promising approaches for environmentally friendly converting $CO_2$ into hydrocarbon fuels. To achieve such an artificial photosynthesis conversion, the development of a high-active photo-catalyst towards $CO_2$ photo-reduction reaction is a prerequisite issue.

Since Inoue *et al.* [1] reported the conversion of $CO_2$ to small amounts of hydrocarbon fuels in the presence of photosensitive semiconductor powders suspended in water as catalysts, various semiconductor photo-catalysts, including oxides [2,3], sulfides [4,5], perovskite [6], carbon nitride [7], metal/covalent organic framework [8–10], *etc.*, had been widely employed to study for the $CO_2$ photo-reduction. Among those semiconductor photo-catalysts, $TiO_2$-based materials are still at the center of attention due to their remarkable stability and suitable band structure [11]. However, pure $TiO_2$ materials usually suffered from the drawback of the rapid recombination of photo-induced electron-hole pairs, which prohibited the transfer of charge carriers and accordingly slowed the photo-catalytic $CO_2$ reduction reaction down, resulting in a low photo-catalytic activity.

As a matter of fact, the $CO_2$ photo-reduction reaction contains three main processes. Firstly, the semiconductor photo-catalysts absorb the light and produce electron-pairs. Then, the electrons and holes would be separated and transfer to the surface of the semiconductor. Lastly, $CO_2$ reduction and $H_2O$ oxidation reactions occur with involving of electrons and holes, respectively. In other words, under the condition of thermodynamic equilibrium, the photo-catalytic $CO_2$ reduction performance is determined by the

* Corresponding author.
*E-mail address:* zhipanwen2016@163.com (Z. Wen).

https://doi.org/10.1016/j.cclet.2021.07.052
1001-8417/

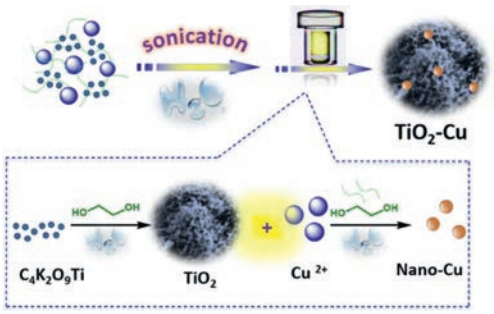


**Fig. 1.** Illustration for the fabrication process and formation mechanism of $TiO_2$-Cu hybrids.

kinetics of the above three processes. [11] Therefore, it is reasonable to promote the capability of $CO_2$ photo-reduction through enhancing the efficiency of one or more of the above three processes during the photo-catalysis reaction.

The past few years, a tremendous flurry of research interest have been devoted onto the surface, interface, and composition engineering of $TiO_2$-based photo-catalysts for enhancing their relatively photo-catalytic activity [12,13]. Especially, continued breakthroughs have been made in the co-catalyst effect [14–17], oxygen vacancy involving [18-22], hetero-junction construction [23–28], *etc*. Among them, coupling with metal co-catalyst [29,30], as one of promising approaches, has attracted more interest thus it can enhance the photo-catalytic performance through promoting the electron–hole separation and migration. For example, Xie *et al*. [31] examined the effect of noble metal co-catalysts and found that the rate of $CH_4$ formation increased in the sequence of Ag < Rh < Au < Pd < Pt, corresponding well to the increase in the efficiency of electron-hole separation. Although most of the published papers revealed that Pt is the most effective co-catalyst to extract photo-generated electrons for $CO_2$ eduction [32–35], Pt element is too rare and expensive to be used in large-scale solar fuels production. Therefore, it is of significance to develop earth-abundant and non-precious materials based co-catalysts for achieving high efficiency of photo-catalytic $CO_2$ reduction.

Based on the above backgrounds and inspired by the challenges, the present study focuses on the solar-driven $CO_2$ photo-reduction activity of nonprecious Cu particle anchored $TiO_2$. Combining with previous work on preparation of hetero-phase $TiO_2$ [36] and Cu-$MO_x$ (M = W, Ti and Ce) [37] nano-composites, a facile one-pot polyol-mediated solvo-thermal approach was employed to successfully prepare $TiO_2$-Cu nano-hybrids. The corresponding photo-catalytic performance was evaluated through $CO_2$ reduction under simulated sunlight irradiation. The contribution of the Cu particles anchored on the $TiO_2$ nano-aggregates to its superior photo-catalytic reduction capability was also studied.

Fig. 1 shows the preparation process of $TiO_2$-Cu composites, which contains the formation of mesoporous $TiO_2$ nanostructure and simultaneous decoration of Cu particle by polyol reduction strategy. The X-ray diffraction (XRD) patterns of the as-synthesized products were displayed in Fig. 2a. It can be found the diffraction peak of the material synthesized without involving of $Cu^{2+}$ precursor could be well indexed with the standard anatase phase $TiO_2$ (JCPDS No. 1-562). After introducing the $Cu^{2+}$ precursor into the reaction system, it was found the as prepared materials were composed of $TiO_2$ and Cu from the XRD diffraction peaks, which correspond well with standard patterns of JCPDS No. 1-562 and 1-1242. Furthermore, with increasing of $Cu^{2+}$ precursor concentration from $TiO_2$-Cu-2.5% to $TiO_2$-Cu-7.5%, the diffraction peak of Cu became stronger. This result suggested that the $TiO_2$-Cu nano-hybrids had been successfully synthesized. As shown in the UV–vis diffuse reflectance spectrum (UV-DRS) of the as-prepared materials (Fig. 2b), an obvious absorption tail could be detected in the visible light region, suggesting that the involving of copper could tailor the light absorption of the materials. As shown in Fig. S1a (Supporting information), when further increased the copper loading amounts, the XRD diffraction peaks of copper in the composites continue growing. At the meantime, as shown in Fig. S1b (Supporting information), the absorption tail of those composites obviously shifted to the visible light region, but the absorption peak intensity below 350 nm become weaker due to the decreased $TiO_2$ amount.

X-ray photoelectron spectroscopy (XPS) was further used to confirm the intrinsic characteristics and chemical states of the as-prepared materials. Take $TiO_2$-Cu-5% as an example, the survey XPS spectrum in Fig. 2c suggests the sample consists of the elements of Ti, O, and Cu. Figs. 2d-f show high-resolution XPS spectra of Ti 2p, O 1s, and Cu 2p, respectively. The binding energy peaks located at 458.5, 459.5, and 464.2 eV belong to the valence states of Ti 2p. The peaks at 529.7 and 531.2 eV of O 1s spectrum (Fig. 2e) are attributed to the formation of Ti-O bonds in $TiO_2$. As displayed in Fig. 2f, the two main peaks at 932.5 and 952.4 eV correspond to the metallic Cu(0) $2p_{3/2}$ and Cu $2p_{1/2}$ state [38], respectively.

The morphology and structure of the as-obtained $TiO_2$ and $TiO_2$-Cu-5% products were shown in Fig. 3a. The $TiO_2$ sample shows morphology of aggregated spherical nanoparticles. With involving of Cu precursor into the reaction system, the obtained $TiO_2$-Cu-5% sample keeps the same morphology (Fig. 3b). However, the energy dispersive X-ray spectroscopy (EDX)-mapping in Figs. 3c-f suggests the material contains the elements of Ti, O, and Cu. TEM images in Figs. 3g-h indicate that both the $TiO_2$ and $TiO_2$-Cu-5% samples comprise many small nano-crystals, leading to a *pseudo*-porous structure. As shown in HRTEM image in Fig. 3i, the lattice fringes of the nanoparticles can be easily identified to be 0.35 and 0.21 nm apart, which is in good agreement with the (101) plane of $TiO_2$ and the (111) plane of Cu, respectively. The above results confirm the successful decoration of Cu nanoparticles on the surfaces of the $TiO_2$ nano-aggregates. The $N_2$ adsorption–desorption isotherms (Fig. S2 in Supporting information) of the $TiO_2$-Cu-5% sample display a distinct Type II hysteresis loop and reveal the typical characteristics of porous materials. The calculated BET surface area is 159.9 $m^2/g$, which corresponds to the average pore sizes of the 9.1 nm.

The photo-catalytic activities of the as-synthesized $TiO_2$ and $TiO_2$-Cu nano-composites were evaluated through solar-driven $CO_2$ reduction in the presence of $H_2O$ vapor under continuous artificial sunlight irradiation. Figs. 4a and b show the $CO_2$ photo-reduction activity and the corresponding evolution rates of the above materials. It was found pure $TiO_2$ could convert $CO_2$ into $CH_4$ and CO products under light irradiation. Furthermore, the involving of proper amounts of copper could enhance the evolution rates of $CH_4$ and CO. When the $TiO_2$-Cu-5% was used as the catalyst, the evolution rates of $CH_4$ and CO were 25.73 and 0.42 μmol $g^{-1}$ $h^{-1}$, respectively, which were significantly promoted comparing with that of pure $TiO_2$ (11.67 and 0.14 μmol $g^{-1}$ $h^{-1}$ for $CH_4$ and CO, respectively). It is clear that the $TiO_2$-Cu-5% present a 2.2 times higher yield of $CH_4$ and 3 times higher CO yield compared with pure $TiO_2$. When further increase the Cu content ($TiO_2$-Cu-7.5%), the $CO_2$ photo-reduction activity decreased and it was attributed to the decrease of $TiO_2$ in such hybrid (Fig. S3 in Supporting information). As shown in Fig. S3, when the loading amount of Cu was 50%, no CO was produced and the $CH_4$ yield of $TiO_2$-Cu-50% was only one tenth of pure $TiO_2$. This is due to that too much Cu could shield light absorption of $TiO_2$ (Fig. S1b). In addition, the XRD pattern of the sample after $CO_2$ photo-reduction was also collected and displayed in Fig. S4 (Supporting information). It was found the composites still showed the main constitute of $TiO_2$ and Cu. But

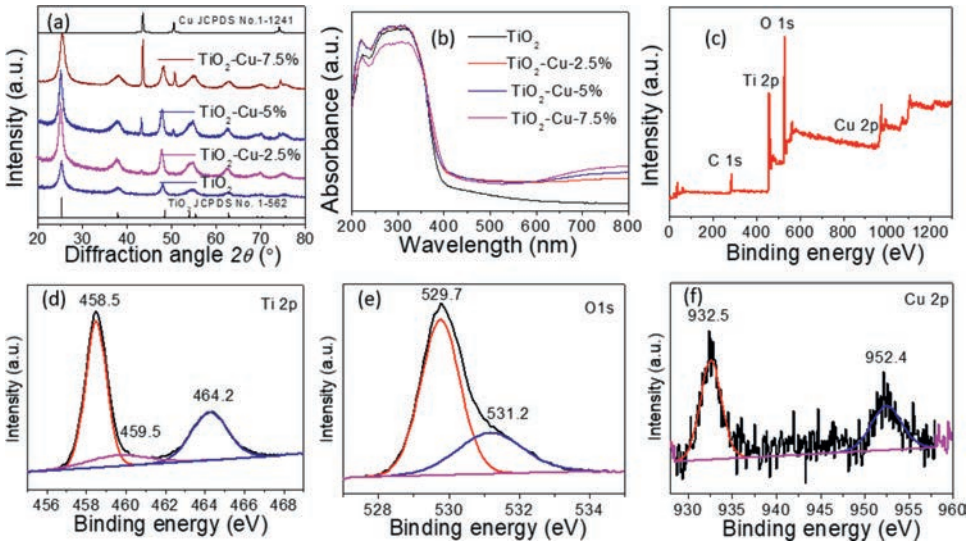


**Fig. 2.** (a) XRD patterns and (b) UV-DRS spectra of $TiO_2$ and $TiO_2$-Cu products. (c) Whole survey, (d) Ti 2p, (e) O 1s and (f) Cu 2p XPS spectra of $TiO_2$-Cu-5%.

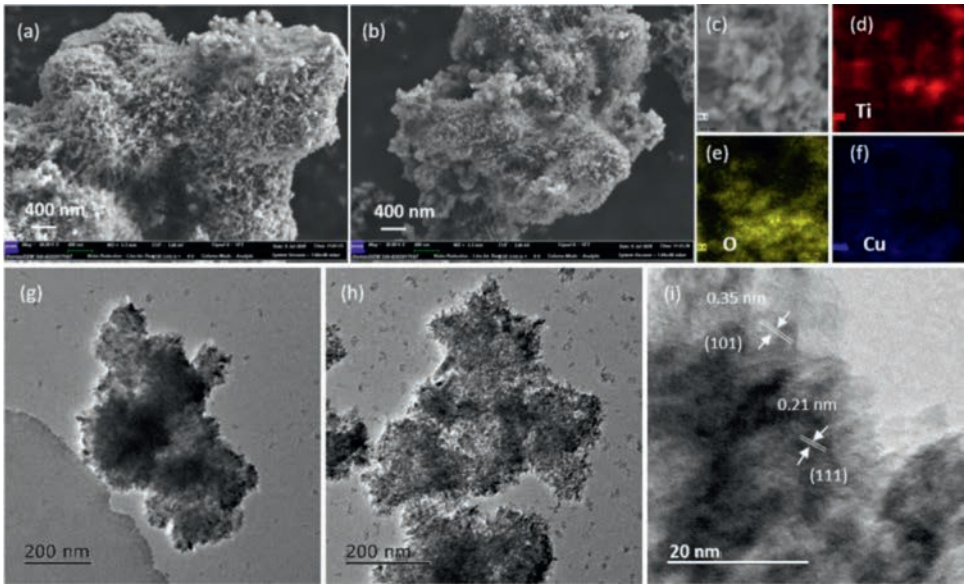


**Fig. 3.** SEM images of $TiO_2$ (a) and $TiO_2$-Cu-5% (b). (c-f) EDX elemental mapping images of $TiO_2$-Cu-5%. TEM image of $TiO_2$ (g). TEM (h) and HRTEM (i) images of $TiO_2$-Cu-5%.

the diffraction peak of $Cu_2O$ also appeared due to the oxidation of Cu by the generated $O_2$ during the photo-catalysis reaction.

It is well-known that proper matching of valence band ($E_{VB}$) and conduction band ($E_{CB}$) sites is important for $CO_2$ photo-reduction. As shown in Fig. 4c, the band gap ($E_g$) of $TiO_2$ was calculated to be 2.89 eV from the Kubelka-Munk function. At the same time, the valence band extreme of $TiO_2$ on the basis of Valence band XPS spectra in Fig. 4d was 2.30 eV. Then, the $E_{CB}$ level from ($E_{VB} - E_g$) was −0.59 eV. Previous studies have pointed out that the potential for reducing $CO_2$ to $CH_4$ and CO in water at a pH value of 7 is −0.24 V ($E_{CO2/CH4}$ = −0.24 V *vs.* NHE) and −0.53 V ($E_{CO2/CO}$ = −0.53 V *vs.* NHE) [39–40], respectively. In this work, the $E_{CB}$ value of $TiO_2$ (corresponding to −0.59 V) was more negative than those values. This indicates that $CH_4$ and CO could be the preferred product.

To better understand the improvement of photo-catalytic activities for the $TiO_2$-Cu nano-composites, the transient photocurrent responses of the as-prepared products were performed to characterize the generation, migration, and recombination of photo-induced electrons and holes. It was clearly observed in Fig. 5a that the photocurrent density of the $TiO_2$-Cu-5% sample electrode was much higher than that of pure $TiO_2$, suggesting a higher separation and lower recombination rate of photo-generated electron-hole pairs in such a hybrid during the photo-catalysis process [41–45]. Photoluminescence (PL) spectra were further used to study the electron-hole separation of the photo-catalyst. As shown in Fig. 5b, the $TiO_2$-Cu-5% sample displayed a lower fluorescence intensity than that of pure $TiO_2$, which indicates a higher separation rate of photo-generated electron and hole pairs during $CO_2$ photo-reduction. Considering the Cu has higher work function than that of $TiO_2$ [14,46,47], the photo-induced electrons in $TiO_2$ would be transferred to the Cu. Meanwhile, the formation of Schottky barrier between $TiO_2$ and Cu resulted from the strong interfacial interaction in the $TiO_2$-Cu nano-composite could promote the transfer and separation of photo-generated electrons.

On the basis of the above analysis, the impact of the Cu particles anchoring on the photo-catalytic $CO_2$ reduction in the $TiO_2$ material was illustrated in Fig. 5c. As mentioned in the photo-reduction test, the photo-catalysts firstly would adsorb a certain amount of $CO_2$ molecules before initiated the Xe lamp, as the ad-

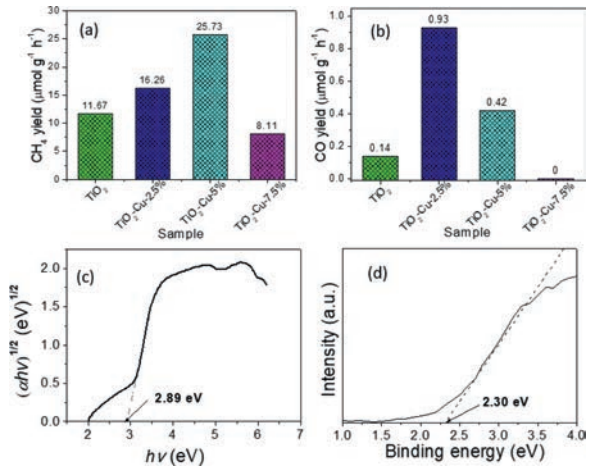


**Fig. 4.** Photo-reduction activity towards the conversion of $CO_2$ into $CH_4$ (a) and CO (b) upon $TiO_2$ and $TiO_2$-Cu nano-composites under simulated solar light irradiation for 4 h. (c) Calculated band gap from UV-DRS spectra of $TiO_2$. (d) Valence band XPS spectra of $TiO_2$.

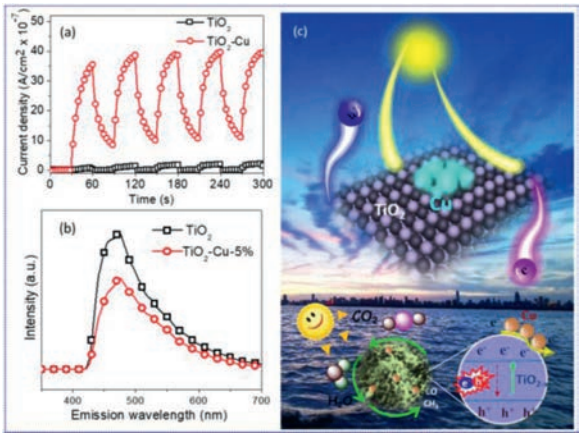


**Fig. 5.** (a) Photocurrent response and (b) PL spectra of $TiO_2$ and the $TiO_2$-Cu-5% nano-composites. (c) Schematic illustration of the charge transfer paths in the $TiO_2$-Cu nano-composite towards $CO_2$ photo-reduction.

sorption is a prerequisite for the occurrence of a photo-catalysis reaction [48–49]. Upon the light irradiation, the $TiO_2$ could absorb the light photons to generate photo-induced electrons and holes. Then, the electrons in the conduction band of $TiO_2$ would be transferred to the surface to engage in the photo-catalytic $CO_2$ reduction for yielding products. In particular, with involving of Cu particles, it would accept the photo-generated electrons from $TiO_2$ and accelerate the rapid charge separation and transfer. As a result, more efficient electron-hole separation in the $TiO_2$-Cu nano-composite was achieved. Finally, the photo-catalytic $CO_2$ reduction to $CH_4$ and CO is significantly enhanced by more photo-generated electrons participating in the photo-catalysis process.

In summary, the $TiO_2$-Cu nano-composite was successfully prepared by a simple polyol approach, which combines the formation of $TiO_2$ nano-aggregates with reduction of $Cu^{2+}$ to Cu. The UV–vis diffuse reflectance and Valence band XPS spectra suggested the prepared $TiO_2$ nano-aggregates had suitable band edge alignment with respect to the $CO_2/CH_4$ and $CO_2$/CO redox potential. Under simulated sunlight irradiation, an enhanced $CH_4$ and CO yield was achieved in the photo-reduction of $CO_2$ using the $TiO_2$-Cu nano-composite. The $TiO_2$-Cu-5% sample exhibits 2.2 times higher $CH_4$ yield and 3 times higher CO yield compared with pure $TiO_2$. This performance enhancement is realized because efficient separation of photo-generated charges was achieved with involving of Cu particles into the $TiO_2$ nano-aggregates. It is expected this work could provide a rational reference for designing efficient and low cost photo-catalysts towards $CO_2$ reduction.

## Declaration of competing interest

The authors declared that they have no conflicts of interest to this work.

## Acknowledgments

This work was supported by the National Natural Science Foundation of China (No. 22102122), the Hubei Provincial Natural Science Foundation (No. 2019CFB386) and the Central Committee Guides Local Science and Technology Development Special Project of Hubei Province (No. 2019ZYYD073).

## Supplementary materials

Supplementary material associated with this article can be found, in the online version, at doi:10.1016/j.cclet.2021.07.052.

## References

[1] T. Inoue, A. Fujishima, S. Konishi, K. Honda, Nature 277 (1979) 637–638.
[2] T. Zhang, J. Low, X. Huang, et al., Chem. Cat. Chem. 9 (2017) 3054–3062.
[3] F. Chen, Z. Ma, L. Ye, et al., Adv. Mater. 32 (2020) 1908350.
[4] M. Zhou, S. Wang, P. Yang, et al., ACS Catal. 8 (2018) 4928–4936.
[5] X. Jiao, X. Li, X. Jin, et al., J. Am. Chem. Soc. 139 (2017) 18044–18051.
[6] R. Shi, G.I.N. Waterhouse, T. Zhang, Sol. RRL 1 (2017) 1700126.
[7] J. Liang, Z. Jiang, P.K. Wong, C.S. Lee, Sol. RRL 5 (2020) 2000478.
[8] R. Li, W. Zhang, K. Zhou, Adv. Mater. 30 (2018) 1705512.
[9] W. Zhong, R. Sa, L. Li, et al., J. Am. Chem. Soc. 141 (2019) 7615–7621.
[10] Z.B. Fang, T.T. Liu, J. Liu, et al., J. Am. Chem. Soc. 142 (2020) 12515–12523.
[11] Y. Ma, X. Wang, Y. Jia, et al., Chem. Rev. 114 (2014) 9987–10043.
[12] T. Kong, Y. Jiang, Y. Xiong, Chem. Soc. Rev. 49 (2020) 6579–6591.
[13] Z. Xiong, Z. Lei, Y. Li, et al., J. Photochem. Photobiol. C 36 (2018) 24–47.
[14] X. Li, J. Yu, M. Jaroniec, X. Chen, Chem. Rev. 119 (2019) 3962–4179.
[15] C. Dong, M. Xing, J. Zhang, Mater. Horizons 3 (2016) 608–612.
[16] A. Meng, L. Zhang, B. Cheng, J. Yu, Adv. Mater. 31 (2019) 1807660.
[17] J. Ran, M. Jaroniec, S.Z. Qiao, Adv. Mater. 30 (2018) 1704649.
[18] W. Fang, L. Khrouz, Y. Zhou, et al., Phys. Chem. Chem. Phys. 19 (2017) 13875–13881.
[19] L. Liu, S. Wang, H. Huang, et al., Nano Energy 75 (2020) 104959.
[20] S. Bai, N. Zhang, C. Gao, Y. Xiong, Nano Energy 53 (2018) 296–336.
[21] M. Ai, J.W. Zhang, Y.W. Wu, et al., Chem. Asian J. 15 (2020) 3599–3619.
[22] Z. Xiu, M. Guo, T. Zhao, et al., Chem. Eng. J. 382 (2020) 123011.
[23] L. Yuan, S.F. Hung, Z.R. Tang, et al., ACS Catal. 9 (2019) 4824–4833.
[24] Z. Xiong, Z. Lei, C.C. Kuang, et al., Appl. Catal. B 202 (2017) 695–703.
[25] K. Li, B. Peng, J. Jin, et al., Appl. Catal. B 203 (2017) 910–916.
[26] J. Zhou, H. Wu, C.Y. Sun, et al., J. Mater. Chem. A 6 (2018) 21596–21604.
[27] S. Jiang, K. Zhao, M. Al-Mamun, et al., Inorg. Chem. Front. 6 (2019) 1667–1674.
[28] W. He, X. Wu, Y. Li, et al., Chin. Chem. Lett. 31 (2020) 2774–2778.
[29] Q. Liu, Q. Chen, T. Li, et al., J. Mater. Chem. A 7 (2019) 27007–27015.
[30] X. Cai, J. Wang, R. Wang, et al., J. Mater. Chem. A 7 (2019) 5266–5276.
[31] S. Xie, Y. Wang, Q. Zhang, et al., ACS Catal. 4 (2014) 3644–3653.
[32] L.Y. Lin, S. Kavadiya, X. He, et al., Chem. Eng. J. 389 (2020) 123450.
[33] M. Tasbihi, F. Fresno, U. Simon, et al., Appl. Catal. B 239 (2018) 68–76.
[34] C. Wang, X. Liu, W. He, et al., J. Catal. 389 (2020) 440–449.
[35] X. Wu, C. Wang, Y. Wei, et al., J. Catal. 377 (2019) 309–321.
[36] J. Xiong, M. Zhang, G. Cheng, J. Colloid Interface Sci. 579 (2020) 872–877.
[37] M. Zhang, J. Xiong, H. Yang, et al., Ind. Eng. Chem. Res. 59 (2020) 15454–15463.
[38] J. Zhu, M. Zhang, J. Xiong, et al., Chem. Eng. J. 375 (2019) 121902.
[39] X. Chang, T. Wang, J. Gong, Energy Environ. Sci. 9 (2016) 2177–2196.
[40] R. Wang, C. He, W. Chen, et al., Chin. Chem. Lett. 32 (2021) 3821–3824.
[41] Y. Wei, G. Cheng, J. Xiong, et al., J. Energy Chem. 32 (2019) 45–56.
[42] Z. Zhou, Y. Li, M. Li, et al., Chin. Chem. Lett. 31 (2020) 2698–2704.
[43] B. Li, L.C. Nengzi, R. Guo, et al., Chin. Chem. Lett. 31 (2020) 2705–2711.
[44] L. Jiang, Y. Xie, F. He, et al., Chin. Chem. Lett. 32 (2021) 2187–2191.
[45] L. Fu, R. Wang, C. Zhao, et al., Chem. Eng. J. 414 (2021) 128857.
[46] S. Xiao, P. Liu, W. Zhu, et al., Nano Lett. 15 (2015) 4853–4858.
[47] X.H. Li, M. Antonietti, Chem. Soc. Rev. 42 (2013) 6593–6604.
[48] M. Zhang, G. Cheng, Y. Wei, et al., J. Colloid Interface Sci. 572 (2020) 306–317.
[49] H. Yang, C. He, L. Fu, et al., Chin. Chem. Lett. 32 (2021) 3202–3206.